Journal of the European Ceramic Society xxx (2017) xxx–xxx

Contents lists available at www.sciencedirect.com

Journal of the European Ceramic Society

journal homepage: www.elsevier.com/locate/jeurceramsoc

Feature article

Fractography of self-glazed zirconia with improved reliability

Zhijian Shen[a,*], Leifeng Liu[a], Xiqing Xu[a], Jing Zhao[a], Mirva Eriksson[a], Yuan Zhong[a], Erik Adolfsson[b], Yihong Liu[c], Andraž Kocjan[d]

[a] Department of Materials and Environmental Chemistry, Arrhenius Laboratory, Stockholm University, S-106 91 Stockholm, Sweden
[b] Swerea IVF, Argongatan 30, S-431 53 Mölndal, Sweden
[c] Department of General Dentistry, Peking University School and Hospital of Stomatology, 100081 Beijing, China
[d] Department for Nanostructured Materials, Jožef Stefan Institute, Jamova 39, SI-1000 Ljubljana, Slovenia

ARTICLE INFO

Article history:
Received 8 December 2016
Received in revised form 2 March 2017
Accepted 3 March 2017
Available online xxx

Keywords:
Fractography
Self-glazed zirconia
Dental restorations
Defects
Nanoceramics

ABSTRACT

The fractography of a new grade of zirconia ceramics, known as self-glazed zirconia, was investigated. The as-sintered intact top surface was made with superior smoothness that mimicked the optical appearances of the natural teeth enamel. The beneath surface opposite to this was made hierarchically rough with microscopic pits of the size up to 60 μm together with grain-level roughness of about 2 μm. The three-point bending test of the samples made with the hierarchically rough surface being tensile one demonstrated an average bending strength of 1120 ± 70 MPa and a Weibull modulus of as high as 18 ascribed to the improved structural homogeneity. Surface topography was found the main origins of crack initiation leading to fracture. The observed unusually predominant transgranular fracture mode of submicron-sized grains disclosed a possible toughening mechanism of disassembling of mesocrystalline grains that differs significantly from the commonly quoted phase transformation toughening of this category of ceramics.

1. Introduction

Zirconia ceramics, commonly in the form of 3 mol-% Y_2O_3 partially stabilized ZrO_2 (3Y-TZP), are increasingly applied for fabrication of dental restorations due to their biocompatibility, mechanical reliability and aesthetic advantages [1–3]. Though zirconia ceramics are known as the toughest family of ceramics [4], clinical failures by fracture have been observed, particularly with the current tendency of adding increased amount of stabilizer in order to increase the content of cubic phase aiming for improving their optical translucency [5,6]. To solve these problems, materials with properties beyond those of ceramics used today must be developed. The general efforts to achieve this have so far mainly been focused on the development of new advanced ceramics and ceramic composites with a drastically reduced grain size [7–9], which has reminded the importance of powder processing in obtaining the required homogeneous microstructure and the key role of processing defects in determining the strength and reliability of ceramic materials [10,11].

Strength measurements are thus usually performed on samples with carefully prepared surfaces to exclude the artificial, extrinsic surface defects introduced by the post-process machining [12]. The strength of a ceramic product containing such extrinsic surface defects is known to be lower than that measured on test bars with carefully prepared surfaces. This means that the material's strength data reported in the literature or obtained from the properties data sheet provided by the manufactures in most of the cases represent only the maximum strength achievable but not that of the components made of such materials. The latter is however essential in predicating the reliability of the ceramic dental restorations having not-polished surfaces with customized geometries. In practice, extrinsic surface defects are further introduced by chairside grinding often required for restoring the demanded occlusion, which in turn would not only increase the surface roughness of the dental prostheses thus the wear of the opposite teeth but also the reliability of the dental prostheses themselves [13,14].

In this work the fracture behaviors of a new grade of self-glazed zirconia prepared by a precision additive 3D gel deposition approach based on hybrid gelation principle were investigated. Self-glazed zirconia was defined as a family of monolithic zirconia ceramics having a superior smooth surface opposite to another hierarchically rough surface both spontaneously formed during the net-shape forming process. While the former is made for imitating

* Corresponding author.
E-mail address: shen@mmk.su.se (Z. Shen).

http://dx.doi.org/10.1016/j.jeurceramsoc.2017.03.008
0955-2219/

the function and optical appearance of natural tooth enamel, the latter is made for enhancing the bonding between ceramic prostheses and natural teeth or abutments above the dental implants [15]. With adjustable optical translucency and aesthetic behaviors the self-glazed zirconia family of ceramics fit particularly for model-free digital workflow of the manufacture of customized full-contour monolithic dental restorations by avoiding conventional manual work of grinding/polishing, veneering and glazing. In practice, their reliability would mainly be determined by the possible fracture initiated on the hierarchically rough surface under tension.

The performed work based on three-point bending test of the samples made with the hierarchically rough surface being tensile one followed by careful electron microscopic fractographic characterization of the fractured surfaces is aiming for disclosing the clues how can a combinational advantage of increased mechanical reliability and improved optical translucency be integrated into this new grade of zirconia ceramics. The fracture behaviors will be correlated to the processing defects with scales span from nanometers up to several tens micrometers, introduced during the entire manufacturing chain from powder synthesis to the sintering of bulk products.

2. Experimental

2.1. Preparation of the test samples

Self-glazed zirconia ceramic test samples were formed by a precision additive 3D gel deposition approach in the similar way as the production of customized self-glazed zirconia dental prostheses, so the samples contained one hierarchically rough surface opposite to the smooth self-glazed surface, both being spontaneously formed during a net-shape forming process based on hybrid gelation principle. All samples were pressure-less sintered in a muffle furnace at 1450 °C for 90 min in air to achieve a relative density above 99.9%. After that, the samples were furnace cooled down to the room temperature. The self-glazed zirconia is a product under development with the commercialization potential thus the processing details can not be disclosed here due to the conflict of interest.

2.2. Characterization of mechanical properties

The as-sintered hierarchically rough surface of 11 bending bars (1.5 × 2 × 30 mm) were evaluated by three-point bending test, using a fixture with a distance of 20 mm between the outer rollers in an universal testing machine (Zwick Z050, Zwick GmbH & Co. KG, Ulm, Germany) at a loading rate of 1 mm/min.

Instrument indentation test was carried out and load-displacement curves were obtained using a Fischerscope H100C nano hardness tester equipped with Vickers diamond indenter. The maximum load of 1 N was applied with the holding time of 10 s.

The hardness and fracture toughness of the sintered samples were measured by a Zwick/Roell ZHV indenter (Zwick/Roenhjll,Ulm, Germany), under a load of 10 kgf with a dwell time of 10 s. The hardness values were determined through the expression listed below [16],

$$H = 1.8544\frac{P}{d^2} \quad (1)$$

where, H is the hardness, P is the applied load, and d is the diagonal of the indentation.

The indentation fracture toughness was then calculated directly from the crack lengths using the equation given by Niihara et al. for Palmqvist cracks [17],

$$K_{IC} = 0.035\left(\frac{l}{a}\right)^{-1/2}\left(\frac{H}{E\Phi}\right)^{-2/5}\left(\frac{Ha^{1/2}}{\Phi}\right) \quad (2)$$

where, Φ is the constraint factor (≈3), E is the elastic modulus (here for zirconia ceramics it is measured to be 234 GPa through instrument indentation test), a is the half-diagonal of the Vickers indent, and l is the crack length measured from the indent edge.

2.3. Phase and microstructure characterization

Phase composition of the as-sintered and fractured surfaces of mechanically tested samples were characterized with X-ray powder diffraction using Panalytical Xpert PRO diffractometer (PANalytical, Almelo, Netherlands) in Bragg-Brentano geometry with Cu-K_α radiation ($\lambda = 1.5418$ Å). Measurements were made over a range of $20^\circ < 2\theta < 80^\circ$. The average crystallite size was determined by Scherrer equation [18]

$$D = k\lambda/B\cos\theta \quad (3)$$

Where, k is a constant rely on particle shape (0.89 for spherical particles), λ is the wave length of the X-ray ($\lambda = 0.154056$ nm for Cu Kα radiation), θ is the diffraction angle and B is the full width at half maximum (FWHM) of diffraction peak.

The microstructure was characterized by using a scanning electron microscope (SEM, JSM-7401F, JEOL, Tokyo, Japan). The as-sintered and fractured samples were washed by water and acetone in an ultrasonic bath before loaded into the SEM and the SEM observation was carried out on the surface without any coating. Accelerating voltages of 1.5 kV was applied in order to reduce the charging up of the samples. Besides, the cross-sections of a green body and an as-sintered sample were polished by Ar ion beam and SEM imaged at accelerating voltages of 8 kV under backscattered electron model to reveal the crystallographic orientation contrast. The grain size of the as-sintered samples was measured using the linear intercept method based on the SEM images (ASTM E0112-10) by the imaging software Smileview, with a three-dimensional correction factor of 1.2. FEI Titan transmission electron microscope (TEM) operating at 300 KV was used for TEM investigation of the zirconia starting powder and sintered bulks.

3. Results and discussion

3.1. Microscopic homogeneity

Fig. 1 shows a low magnification optical microscopic image and a high magnification SEM micrograph taken on the as sintered hierarchically rough surface of a tested sample. It appears that while the material is dense with rather homogeneous and fine grained microstructure, this surface reveals a hierarchically rough surface topography containing microscopic pits with size up to 60 μm and grain-level roughness of about 2 μm. The measured average grain size on this surface is 310 ± 90 nm.

Fig. 2 shows two backscattered SEM micrographs taken on Ar ion beam polished cross-section of a green body after burning-off organic binder and on a pressure-less sintered test sample, respectively. A homogeneous close packing of the starting nanoparticles achieved in the green stage is clearly demonstrated in Fig. 2(a). The low coordination number of uniformly distributed individual voids noticeable in this image would indicate a superior sinterablity of the obtained green body formed *via* such a precision additive 3D gel deposition approach. The fact that there are only fewer nano-sized residual pores visible on the Ar ion beam polished cross-section of the sintered test sample (see Fig. 2(b)) confirms that full densification is achieved by pressure-less sintering. An average grain size of 250 ± 70 nm is determined on the polished cross-section of the as-sintered sample, which is smaller than that observed on the as-sintered tensile surface. The enhanced surface atomic diffusion on free surfaces stimulated by optical radiation at high temperature

Please cite this article in press as: Z. Shen, et al., Fractography of self-glazed zirconia with improved reliability, *J Eur Ceram Soc* (2017), http://dx.doi.org/10.1016/j.jeurceramsoc.2017.03.008

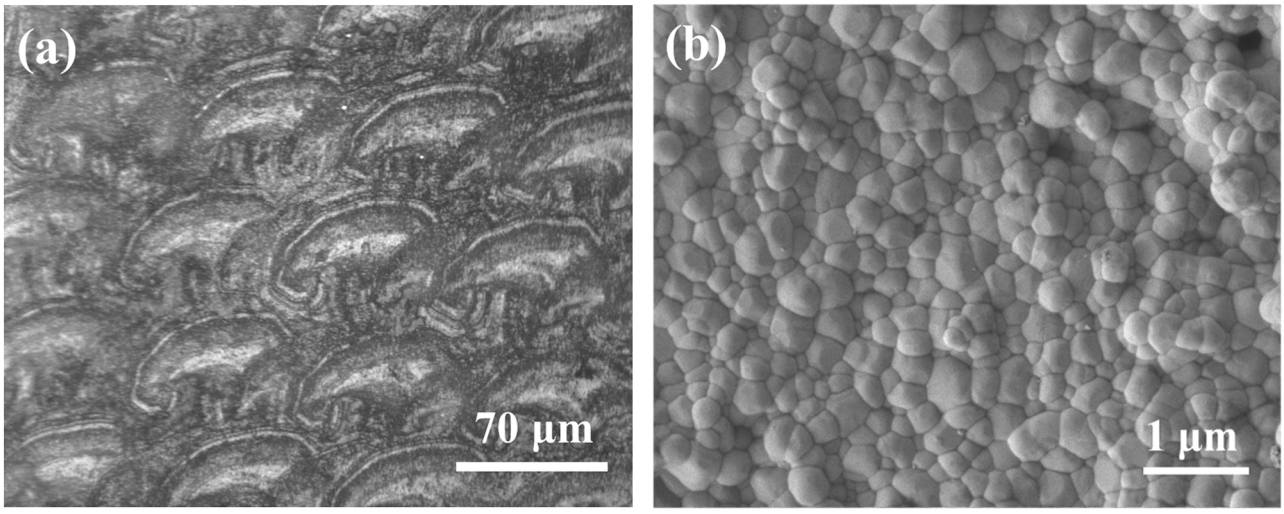

Fig. 1. An optical microscopic image (a) and a SEM micrograph (b) taken on as-sintered hierarchically rough surface of the test sample prepared by pressure-less sintering.

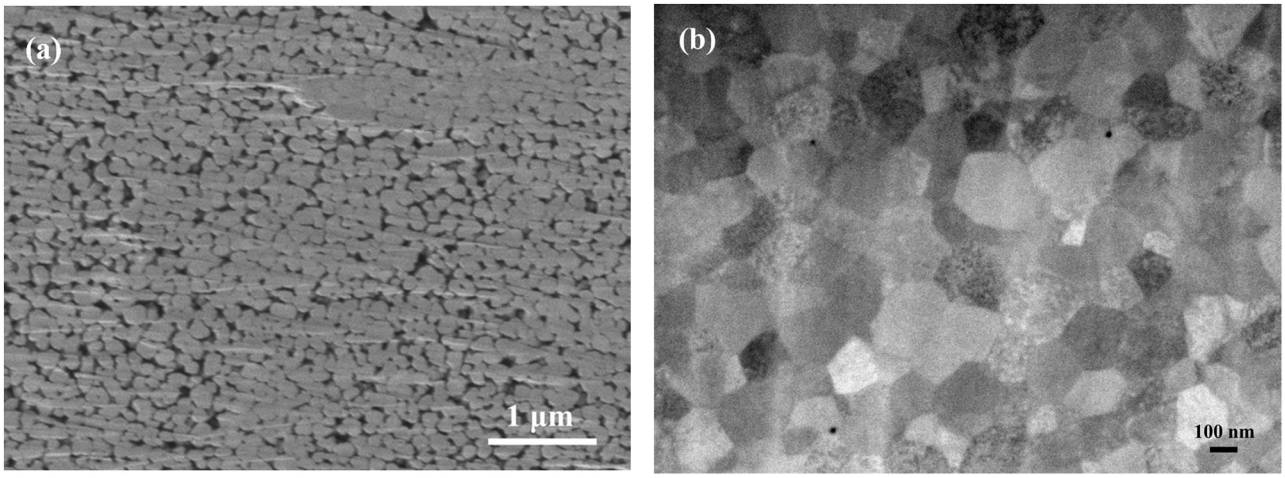

Fig. 2. Backscattered SEM micrographs taken on Ar ion beam polished cross-section of a green body after burning-off organic binder (a) and a pressure-less sintered test sample (b).

may be the origin of the observed increased grain growth rate on the sample surface [19].

The observation of apparent contrasts inside each individual grains in Fig. 2(b) is intriguing. Normally, the contrasts observed in backscattered electron images are interpreted to be formed by differences either of the chemical composition or of the crystallographic orientation. Thus, the contrasts among adjacent grains may be interpreted to be the result of their different crystallographic orientation. However, it is not straightforward to understand where the contrasts inside each individual grains comes from, as zirconia ceramics are, by definition, polycrystalline materials composed of many randomly orientated grains in which each individual grain should be regarded as a small single crystal.

TEM investigation was therefore performed to closely check the intra-granular structure. Fig. 3 shows two TEM images taken on the starting powder and sintered bulk, respectively. As illustrated in Fig. 3(a), the individual nano-particles in the starting powder appear to be secondary particle agglomerates composed of even smaller nano-sized primary crystallites. Two types of boundaries between the adjacent nano-crystallites are observed in the sintered bulk, namely, large angle and small angle boundaries indicated by dashed elliptic and rectangular loops, respectively, in Fig. 3(b). The former may be interpreted as a grain boundary between two adjacent grains in the usual sense, whereas the later may represent the type of intra-granular boundaries with small lattice mismatch between two adjacent nano-crystallites inside an individual grain of single-crystal signature in general. This characteristic assembling feature of nano-sized primary crystallites inside each nano-grain reveals a possible mechanism of ordered coalescence of nanocrystals, which may be valid in the present case operating during the conventional sintering of consolidated bulks [20,21].

In our previous work we have demonstrated the benefit of assembling nano-sized crystallites into coarser, yet nanostructured, mesocrystalline powder in promoting densification and grain growth *via* ordered coalescence of primary nano-crystallites [22]. The ordered coalescences of several nano-sized crystallites with random orientation allow them to form a larger mesocrystalline grain of single crystal signature. In this non-classical grain growth process, nanocrystalline particles themselves act as building blocks to be assembled and form the larger grains in a coherent manner by involving crystallite migration, crystallographic reorientation and coherent assembly of nano-sized primary crystallites. Any imperfect coalescence between them would then give rise to the quasi-interfaces inside grown-up mesocrystalline grains of single-crystal signature. The quasi-interfaces may appear as the aggregation of point or line defects like vacancy arrays or aggre-

Please cite this article in press as: Z. Shen, et al., Fractography of self-glazed zirconia with improved reliability, *J Eur Ceram Soc* (2017), http://dx.doi.org/10.1016/j.jeurceramsoc.2017.03.008

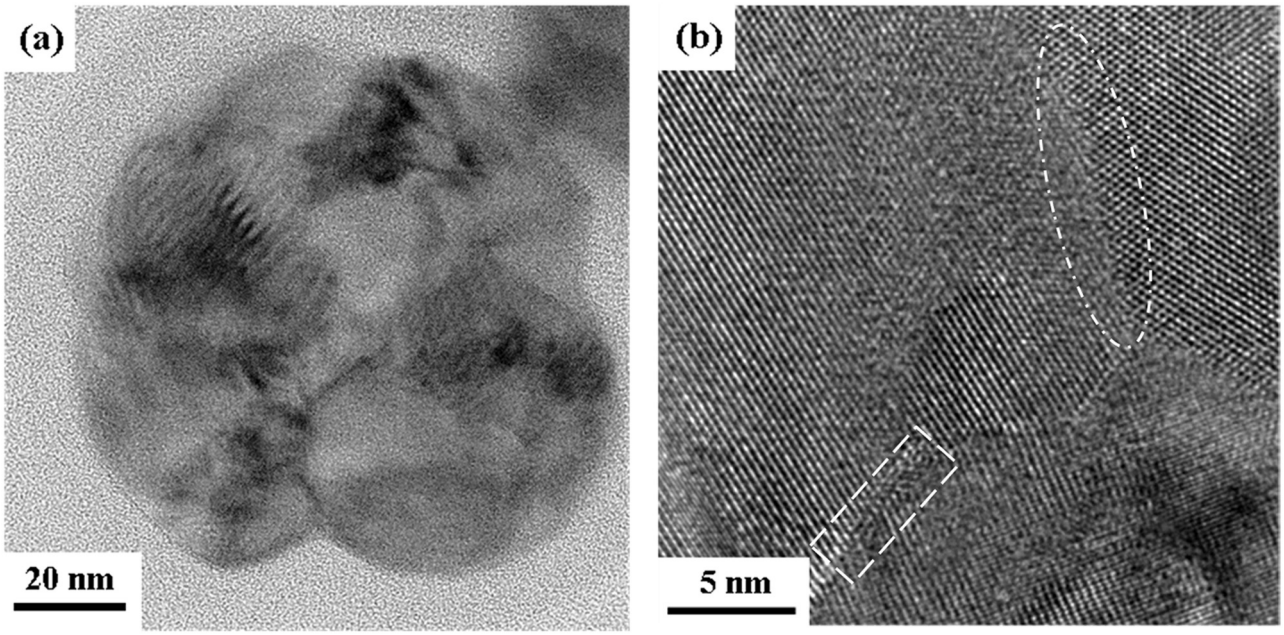

Fig. 3. TEM micrographs taken on the starting powder (a) and on an as-sintered sample (b) revealing the presence of atomic-level structural defects inside individual particles/grains.

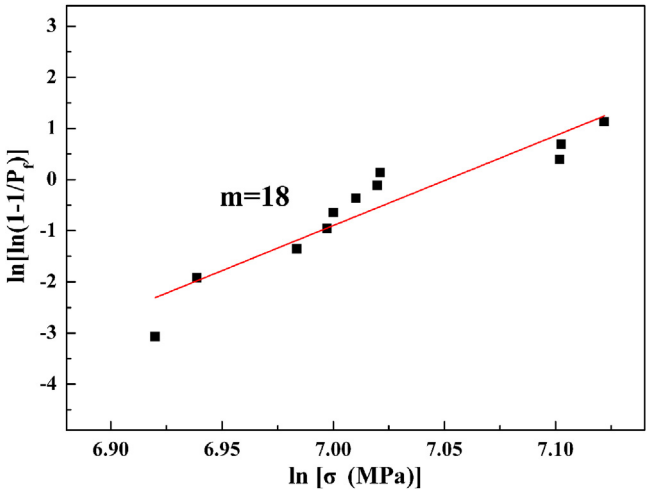

Fig. 4. Weibull plots of the bending strength determined by three-point bending test.

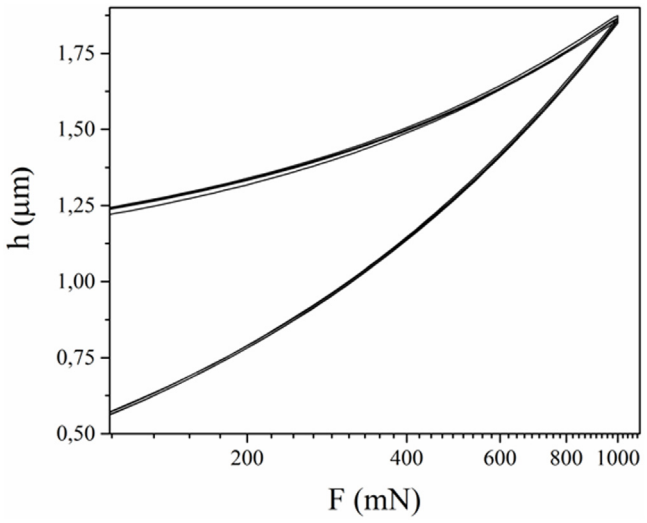

Fig. 5. A load–displacement curve recorded during the nano-indentation test.

gated dislocations as those revealed in Fig. 3. The formation of quasi-interfaces provides a new tool for interfacial engineering in polycrystalline materials [20].

3.2. Mechanical properties

Table 1 lists the determined mechanical properties of the self-glazed zirconia ceramic samples. A Vickers hardness of 12.9 ± 0.1 GPa and an average bending strength of 1120 ± 70 MPa confirm that the sintered bulk is dense and with fine grained microstructure.

A high Weibull modulus of 18 was extracted from the Weibull plot of the bending strength, as shown in Fig. 4. Considering that the Weibull modulus was determined using only 11 specimens, the unbiased estimators for the Weibull modulus should be developed. In the work of Tiryakioglu [23], the distribution of Weibull parameter was found to be normal by using the Anderson-Darling goodness-of-fit test, and the confidence intervals on Weibull modulus could be demonstrated. Based on the percentage points for the distribution of m_{true}, the true value of Weibull parameter lies between 10 and 34 with 95% confidence. The high value of Weibull modulus reveals the improved reliability of the tested samples with extremely narrow distribution of critical flaw population [24].

It is believed that the superior mechanical properties are closely related to their fine grained structure with improved homogeneity. From the slope of the unloading curve of a load-displacement trace recorded *via* nanoindentation test, as shown in Fig. 5, the Young's modulus of the sample can be determined. A Young's modulus value of 234 GPa determined, which is slightly higher than those reported in literature [25], can probably be again attributed to the fine grained microstructure. Moreover, an indentation fracture toughness of 5.2 ± 0.2 MPa.m$^{1/2}$ for a ceramic sample with nano-grained microstructure calls further understanding of the toughening mechanism.

Please cite this article in press as: Z. Shen, et al., Fractography of self-glazed zirconia with improved reliability, J Eur Ceram Soc (2017), http://dx.doi.org/10.1016/j.jeurceramsoc.2017.03.008

Table 1
Summary of the measured mechanical properties.

Av. Grain Size (nm)	H_V10 (GPa)	K_{IC} (MPa $m^{1/2}$)	Bending Strength (MPa)	Young's modulus (GPa)
310 ± 90	12.9 ± 0.1	5.2 ± 0.2	1120 ± 70	234

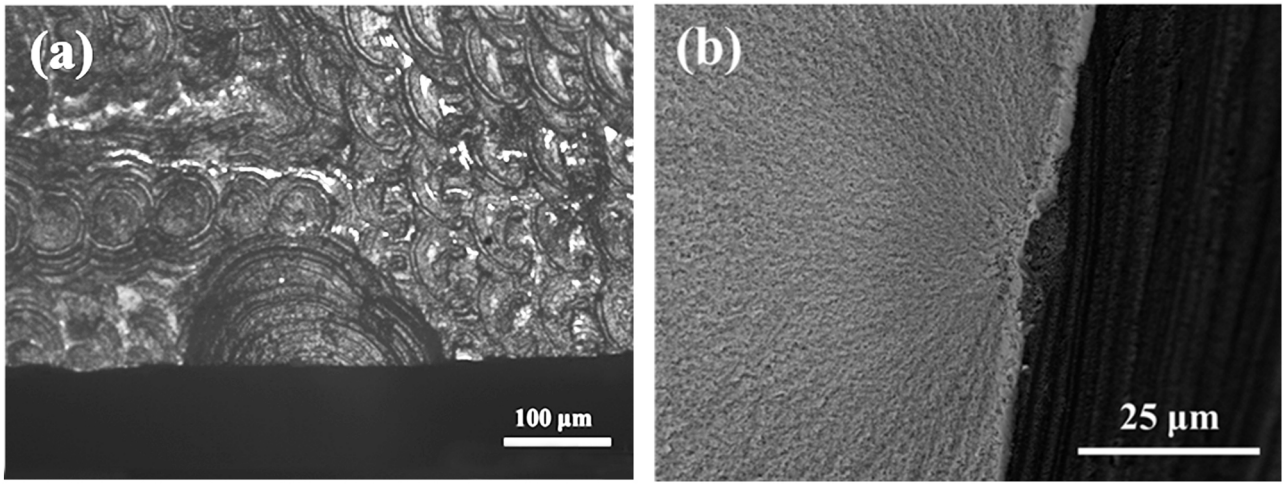

Fig. 6. An optical microscopic image and a SEM micrograph taken on the tensile surface (a) and on the surface perpendicular to the tensile surface (b), respectively, revealing the surface local microscopic pits of the samples are the main origins of fracture.

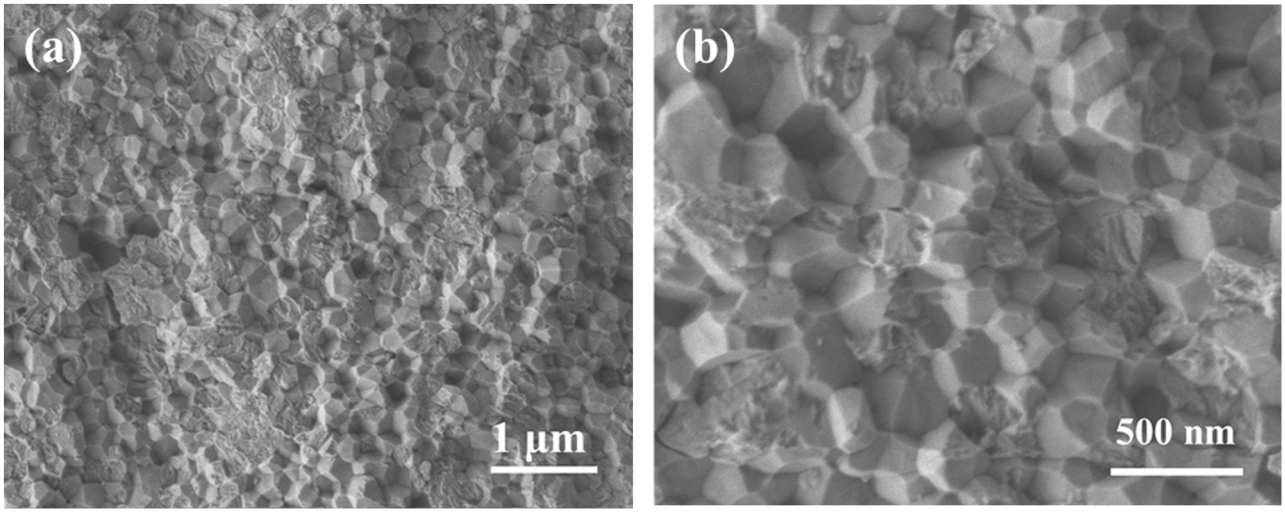

Fig. 7. SEM images taken on the fracture surface.

3.3. *Fractography and fracture origins*

Fig. 6 shows an optical microscopic image taken on the tensile surface (a) and an SEM micrograph of the newly formed fracture surface perpendicular to the tensile surface (b) after three-point bending test. It appears evident that the surface local microscopic pits, formed by purpose or introduced as the type of processing defects, are the main origins of crack initiation leading to fracture. Their size would thus determine the strength [10,11].

It is worthy to note that most of such surface features/defects might be minimized through careful surface treatment, e.g. polishing, that would yield further improved strength and Weibull modulus, which, however, does not always reflect the production and application condition of dental ceramic prostheses, *e.g.* crowns and bridges. Bending strength measured on as-sintered hierarchically rough surface appears more relevant in the current case of self-glazed zirconia, as when this concept is applied for model-free manufacture of customized full-contour monolithic dental restorations, *e.g.* crowns and bridges. An as-sintered hierarchically rough surface with surface topography as revealed by Fig. 1 is needed and would be used directly to enhance bonding between ceramic prostheses and natural teeth or abutments above the dental implants.

Fig. 7 shows the SEM images taken on the fracture surface with high magnification. It reveals the co-existence of intergranular and transgranular fracture. The former resulted faceted grains morphology, whereas the later ended up a fairly rough looking fracture surface across the individual grains. The determined average grain size on the fracture surface is about 260 ± 70 nm, similar to the value observed on polished cross-section as shown in Fig. 2(b). In general, nanocrystalline ceramics have high strength with intergranular facture as the most common fracture mode [26,27]. Transgranular fracture has rarely been reported in fine-grained ceramics until very recently when a small amount of alumina was introduced into the 3Y-TZP, which sufficiently increased the trans-

Please cite this article in press as: Z. Shen, et al., Fractography of self-glazed zirconia with improved reliability, *J Eur Ceram Soc* (2017), http://dx.doi.org/10.1016/j.jeurceramsoc.2017.03.008

granular type of fracture as compared to the alumina-free 3Y-TZP [28]. In this case, the fractured grains seemed to be mesocrystalline, that is, composed of assembled intragranular nano-crystallites. The observed intragranular structure on the fractured surface may be linked directly to the unusual assembling feature of the individual mesocrystalline grains discussed above in 3.1. It is suggested that the frequent transgranular type of fracture of submicron sized grains is probably resulted from the disassembling of mesocrystalline grains, and this unusual fracture mode would disclose a new possible toughening mechanism.

3.4. Toughening by disassembling of mesocrystalline grains

It was puzzling to explain such experimental results that an indentation fracture toughness up to 5.2 ± 0.2 MPa $m^{1/2}$ in a zirconia nanoceramic sample was achieved under the condition of almost no phase transformation until we observed the unusual transgranular type of fracture feature in more than half of the grains. Here, we would propose the toughening mechanism based on disassembling of mesocrystalline grains. Assuming most of the grains in a nanoceramic sample are mesocrystalline, *i.e.* being composed of assembled intra-granular crystallites among which small angle lattice mismatch and atomic-level defects commonly exist, during the fracture of such sample it is highly possible that the mesocrystalline grains would be broken by the propagating cracks, yielding the transgranular type of fracture. The disassembling of mesocrystalline grains leads to more frequent crack deflection that alone or together with absorbing more fracture energy would thus contribute to the increase of fracture toughness.

Until now individual grains in nanoceramics have been regarded as single crystals, thus are extremely difficult to be broken by the propagating cracks. This expectation is supported by the usual experimental observation that intergranular fracture is the common fracture mode, whereas transgranular fracture has been rarely reported in nanoceramics [25,26]. The toughening mechanism emphasized here seems to break the strength-toughness trade-off stating that reducing grain size would always increase the bending strength at the expense of reducing fracture toughness. This toughening mechanism thus would bear more general implication for developing tougher nanoceramics. As long as mesocrystalline grains are built up by assembled nano-crystallites with slightly mismatched crystallographic orientations, the intragranular boundaries have the potential to act as weak interfaces for crack propagation and deflection in general. In combination with already proven concept, *e.g.* making t-ZrO_2 more transformable by reducing the concentration of stabilizer, further exploiting the potential of this new toughening mechanism would lead to the emerging of even tougher and stronger zirconia nanoceramics. More detailed investigation on microstructure to reveal the disassembling process is certainly needed to gain a better understanding of this new toughening mechanism.

Fig. 8 shows the XRD patterns recorded on the as-sintered and fractured surfaces, which prove the t-ZrO_2 as the dominate phase on both surfaces. On the as-sintered surface there is no detectable monoclinic phase, whereas very weak characteristic peaks of m-ZrO_2 emerge on the fracture surface. The comparison in the XRD patterns suggests that during fracture the contribution of phase transformation of t- to m-ZrO_2 to toughening is surprisingly negligible. It was shown that for conventionally sintered zirconia at 1450 °C for 2 h having a grain size of about 0.3 μm, more than 20 wt% of monoclinic phase was detected on the fracture surface [29]. It is well known, that the stress-induced phase transformation of ZrO_2 from t- to m-ZrO_2 is associated with a shear transformation strain of ~16% and a corresponding ~4% volume change, which can block the crack propagation and prevent fracture, leading to high toughness [30,31]. In the current case, the martensitic phase

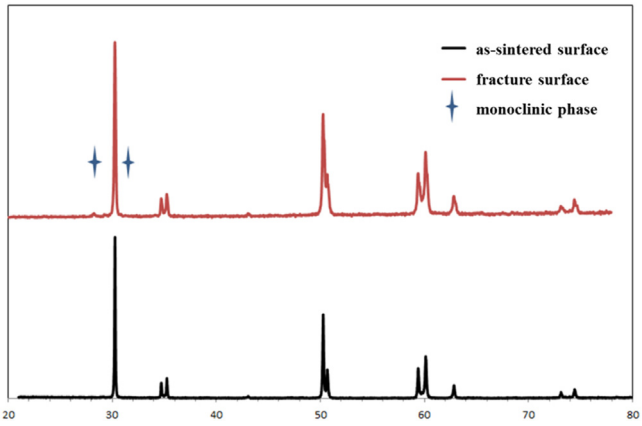

Fig. 8. XRD patterns recorded on as-sintered and fracture surfaces.

transformation of ZrO_2 appears, however, being prevented most probably by reduced size of grains (or nanocrystalline domains) with a consistent stabilizer Y_2O_3 concentration of 3 mol% [31,32]. By using the Scherrer equation and assuming the material was free of the cubic phase, the crystallite size is calculated, being 88 nm on the as-sintered surface and 49 nm on the fracture surface. The apparent reduction of measured crystallite size is a result of disassembling of mesocrystalline grains during fracture rather than stress induced phase transformation.

4. Conclusions

In summary, it is shown that a new grade of zirconia ceramics, known as self-glazed zirconia nanoceramics, prepared by a precision additive 3D gel deposition approach based on hybrid gelation principle, demonstrates improved structural homogeneity and balanced mechanical properties: Bending strength 1120 ± 70 MPa; Weibull modulus of 18; fracture toughness of 5.2 ± 0.2 MPa $m^{1/2}$; hardness of 12.9 ± 0.1 GPa and Young's modulus of 234 GPa. Measuring bending strength on as-sintered hierarchically rough surface but not on well-polished surface appears more indicative and relevant for guiding the application of self-glazed zirconia ceramics for model-free manufacture of customized full-contour dental restorations, for which an as-sintered rough surface is demanded, on which the local microscopic pits, formed by purpose or introduced as the type of processing defects, are confirmed to be the main origins of crack initiation leading to fracture. The observed frequent and unusual transgranular fracture of submicron sized grains disclosed a possible toughening mechanism of disassembling of mesocrystalline grains that differs significantly from the commonly quoted phase transformation toughening of this category of ceramics. The toughening mechanism emphasized here seems to break the strength-toughness trade-off stating that reducing grain size would always increase the bending strength at the expense of reducing fracture toughness. Further exploiting the potential of this new toughening mechanism would lead to the emerging of even tougher and stronger zirconia nanoceramics.

Acknowledgements

This work was supported by Berzelii Center EXSELENT on Porous Materials that is a joint initiative to promote excellent, multidisciplinary and innovative research on porous materials and sponsored by the Swedish Governmental Agency for Innovation Systems (Vinnova) and the Swedish Research Council (VR) through the grant 2015-02316. Slovenian Research Agency is also acknowledged for

funding the research program Engineering and bio-ceramics (P2-0087).

References

[1] J. Chevalier, L. Gremillard, S. Deville, Low-temperature degradation of zirconia and implications for biomedical implants, Annu. Rev. Mater. Res. 37 (2007) 1–32.
[2] E. Camposilvan, F.G. Marro, A. Mestra, M. Anglada, Enhanced reliability of yttria-stabilized zirconia for dental applications, Acta Biomater. 17 (2015) 36–46.
[3] Y. Xiong, Z. Fu, V. Pouchly, K. Maca, Z. Shen, Preparation of transparent 3Y-TZP nanoceramics with no low-temperature degradation, J. Am. Ceram. Soc. 97 (2014) 1402–1406.
[4] R.H.J. Hannink, P.M. Kelly, B.C. Muddle, Transformation toughening in zirconia containing ceramics, J. Am. Ceram. Soc. 83 (2000) 461–487.
[5] L. Hallmanna, P. Ulmerb, E. Reusserb, M. Louvelb, C.H.F. Hämmerle, Effect of dopants and sintering temperature on microstructure and low temperature degradation of dental Y-TZP-zirconia, J. Eur. Ceram. Soc. 32 (2012) 4091–4104.
[6] H. Tong, C.B. Tanaka, M.R. Kaizer, Y. Zhang, Characterization of three commercial Y-TZP ceramics produced for their high-translucency, high-strength and high-surface area, Ceram. Int. 42 (2016) 1077–1085.
[7] J. Chevalier, A.H. De-Aza, G. Fantozzi, M. Schehl, R. Torrecillas, Extending the lifetime of ceramic orthopaedic implants, Adv. Mater. 12 (2000) 1619–1621.
[8] R.J. Kohal, M. Bächle, A. Renz, F. Butz, Evaluation of alumina toughened zirconia implants with a sintered, moderately rough surface: an experiment in the rat, Dent. Mater. 32 (2016) 65–72.
[9] Y.M. Kong, H.E. Kim, H.W. Kim, Production of aluminum–zirconium oxide hybridized nanopowder and its nanocomposite, J. Am. Ceram. Soc. 90 (2007) 298–302.
[10] J.B. Wachtman, W.R. Cannon, M.J. Matthewson, Mechanical Properties of Ceramics, second edition, John Wiley & Sons, Inc, Hoboken, USA, 2009.
[11] J.D. Hogana, L. Farbaniec, T. Sano, M. Shaeffer, K.T. Ramesh, The effects of defects on the uniaxial compressive strength and failure of an advanced ceramic, Acta Mater. 102 (2016) 263–272.
[12] A.R. Alao, R. Stoll, X.F. Song, T. Miyazaki, Y. Hotta, Y. Shibata, L. Yin, Surface quality of yttria-stabilized tetragonal zirconia polycrystal in CAD/CAM milling, sintering, polishing and sandblasting processes, J. Mech. Behav. Biomed. Mater. 65 (2017) 102–116.
[13] T.A. Sulaiman, A.A. Abdulmajeed, T.E. Donovan, L.F. Cooper, R. Walter, Fracture rate of monolithic zirconia restorations up to 5 years: a dental laboratory survey, J. Prosthet. Dent. 116 (2016) 436–439.
[14] P. Pittayachawan, A. McDonald, A. Young, J.C. Knowles, Flexural strength, fatigue life, and stress-induced phase transformation study of Y-TZP dental ceramic, J. Biomed. Mater. Res. B 88 (2009) 366–377.
[15] Y. Liu, Y. Wang, D. Wang, J. Ma, L. Liu, Z. Shen, Self-glazed zirconia reducing the wear to tooth enamel, J. Eur. Ceram. Soc. 36 (2016) 2889–2894.
[16] A. Bravo-Leon, Y. Morikawa, M. Kawahara, M.J. Mayo, Fracture toughness of nanocrystalline tetragonal zirconia with low yttria content, Acta Mater. 50 (2002) 4555–4562.
[17] K. Niihara, R. Morena, D.P.H. Hasselman, Evaluation of K_{IC} of brittle solids by the indentation method with low crack-to-indent ratios, J. Mater. Sci. Lett. 1 (1982) 13–16.
[18] P. Scherrer, N.G.W. Gottingen, Math-Phys. Kl. 2 (1918) 96–100.
[19] D. Salamon, R. Kalousek, J. Zlámal, K. Maca, Role of conduction and convection heat transfer during rapid crack-free sintering of bulk ceramic with low thermal conductivity, J. Eur. Ceram. Soc. 36 (2016) 2955–2959.
[20] J. Hu, Z. Shen, Grain growth by multiple ordered coalescence of nanocrystals during spark plasma sintering of $SrTiO_3$ nanopowders, Acta Mater. 60 (2012) 6405–6412.
[21] D. Salamon, K. Maca, Z. Shen, Rapid sintering of crack-free zirconia ceramics by pressure-less spark plasma sintering, Scripta Mater. 66 (2012) 899–902.
[22] A. Kocjan, V. Pouchly, Z. Shen, Processing of zirconia nanoceramics from a coarse powder, J. Eur. Ceram. Soc. 35 (2015) 1285–1295.
[23] M. Tiryakioglu, D. Hudak, Unbiased estimates of the Weibull parameters by the linear regression method, J. Mater. Sci. 43 (2008) 1914–1919.
[24] J. Tinschert, D. Zwez, R. Marx, K.J. Anusavice, Structural reliability of alumina-, feldspar-, leucite-, mica- and zirconia-based ceramics, J. Dent. 28 (2000) 529–535.
[25] D. Munz, T. Fett, Ceramics-Mechanical Properties, Failure Behaviour Materials Selection, Springer, Heidelberg, 2001.
[26] V.V. Srdic, M. Winterer, H. Hahn, Sintering behavior of nanocrystalline zirconia prepared by chemical vapor synthesis, J. Am. Ceram. Soc. 83 (2000) 461–487.
[27] U. Anselmi-Tamburini, J.N. Woolman, Z.A. Munir, Transparent nanometric cubic and tetragonal zirconia obtained by high-pressure pulsed electric current sintering, Adv. Funct. Mater. 17 (2007) 3267–3273.
[28] A. Samodurova, A. Kocjan, M.V. Swain, T. Kosmac, The combined effect of alumina and silica co-doping on the ageing resistance of 3Y-TZP bioceramics, Acta Biomater. 11 (2015) 477–487.
[29] L. Ruiz, M. Readey, Effect of heat treatment on grain size, phase assemblage, and mechanical properties of 3 mol% Y-TZP, J. Am. Ceram. Soc. 79 (1996) 2331–2340.
[30] R.C. Garvie, R.H.J. Hannink, R.T. Pascoe, Ceramic steel? Nature 258 (1975) 703–704.
[31] J. Chevalier, L. Gremillard, A.V. Virkar, D.R. Clarke, The tetragonal-monoclinic transformation in zirconia: lessons learned and future trends, J. Am. Ceram. Soc. 92 (2009) 1901–1920.
[32] P.F. Becher, M.V. Swain, Grain-size-dependent transformation behavior in polycrystalline tetragonal zirconia, J. Am. Ceram. Soc. 75 (1992) 493–502.

Please cite this article in press as: Z. Shen, et al., Fractography of self-glazed zirconia with improved reliability, *J Eur Ceram Soc* (2017), http://dx.doi.org/10.1016/j.jeurceramsoc.2017.03.008